2-17-2001

Pulmonary arterial remodeling revealed by microfocal x-ray tomography

Kelly L. Karau
College of Wisconsin

Robert C. Molthen
Marquette University, robert.molthen@marquette.edu

Anita H. Dhyani
Marquette University

Steven Thomas Haworth
Medical College of Wisconsin

Christopher A. Dawson
Medical College of Wisconsin

Published version. Published as part of the proceedings of the conference, *SPIE 4321, Medical Imaging 2001: Physiology and Function from Multidimensional Images*, 2001: 282-287. DOI.

Pulmonary arterial remodeling revealed by microfocal x-ray tomography

Kelly L. Karau*[a,b], Robert C. Molthen[a,c], Roger H. Johnson[a,c], Anita H. Dhyani[a],
Steven T. Haworth[b] and Christopher A. Dawson[a,b,c]
[a]Marquette University, [b]Medical College of Wisconsin and [c]Zablocki VAMC

ABSTRACT

Animal models and micro-CT imaging are useful for understanding the functional consequences of, and identifying the genes involved in, the remodeling of vascular structures that accompanies pulmonary vascular disease. Using a micro-CT scanner to image contrast-enhanced arteries in excised lungs from fawn hooded rats (a strain genetically susceptible to hypoxia induced pulmonary hypertension), we found that portions of the pulmonary arterial tree downstream from a given diameter were morphometrically indistinguishable. This "self-consistency" property provided a means for summarizing the pulmonary arterial tree architecture and mechanical properties using a parameter vector obtained from measurements of the contiguous set of vessel segments comprising the longest (principal) pathway and its branches over a range of vascular pressures. This parameter vector was used to characterize the pulmonary vascular remodeling that occurred in rats exposed to a hypoxic (11.5% oxygen) environment and provided the input to a hemodynamic model relating structure to function. The major effect of the remodeling was a longitudinally (pulmonary artery to arterioles) uniform decrease in vessel distensibility that resulted in a 90% increase in arterial resistance. Despite the almost uniform change in vessel distensibility, over 50% of the resistance increase was attributable to vessels with unstressed diameters less than 125 microns.

Keywords: pulmonary arterial tree, fawn hooded rat, computed tomography, microfocal imaging, self-consistent, hemodynamic model, vascular resistance

1. INTRODUCTION

To better understand the mechanisms of disease progression and the efficacy of interventions there is a need to develop and refine imaging methods for phenotyping rodent models of complex traits associated with pulmonary hypertension. To investigate pulmonary arterial tree structure-function in this context, we utilize a high resolution micro-CT scanner for imaging the pulmonary arterial tree in excised rat lungs.

Three-dimensional (3D) volumetric images provide a complex pulmonary arterial tree data set. Because the pulmonary arterial tree is comprised of several hundred thousand vessel segments[1,2,3], it is not practical to include measurements of each segment in the quantitative description of the tree. Instead, it is desirable to produce a morphometric summary of the tree, including a graphical and algebraic representation that can be reproduced in a practical and robust fashion and that retains the hemodynamically significant characteristics of the whole tree. The approach taken to summarize the pulmonary arterial trees in this study is based on the self-consistency concept wherein all portions of the tree downstream from a given diameter vessel are considered statistically equivalent[4]. The summary is obtained by measuring only the diameters of the larger trunk vessel and the smaller branch at each bifurcation and the distances between bifurcations along the main trunk (the single longest pathway) of the pulmonary arterial tree, beginning at the pulmonary artery and ending with the terminal arteriole[5]. The measurements are the input to a mathematical model that describes the whole tree structure. The result of performing these measurements is a parameter vector that can be used to make quantitative comparisons of the complex image data sets from animals with normal and abnormal pulmonary circulations. In addition, it can be the input to a hemodynamic model relating structure and function.

In what follows, we demonstrate the process by comparing pulmonary arterial tree architecture and mechanics in fawn hooded rats (a strain genetically susceptible to hypoxia-induced pulmonary hypertension) from which the lungs were removed after 3 weeks in an exposure chamber with inspired O_2 of 21.0% (normoxic) or 11.5% (hypoxic).

2. METHODOLOGY

2.1 Lung Preparation

After the normoxic or hypoxic exposure, each rat was anesthetized with pentobarbital sodium (40 μg/g body weight i.p.), the trachea clamped, and the chest opened. Heparin (200 IU in 0.2 ml) was administered via injection into the right

Medical Imaging 2001: Physiology and Function from Multidimensional Images, Chin-Tu Chen, Anne V. Clough, Editors, Proceedings of SPIE Vol. 4321 (2001) © 2001 SPIE · 1605-7422/01/$15.00

ventricle. The pulmonary artery was cannulated with a saline filled catheter (polyethylene tubing 1.67 mm i.d. 2.42 mm o.d.) via the conus arteriosis and the heart dissected away. The lungs were removed from the chest, and suspended from the cannulated trachea and the pulmonary arterial catheter. The lungs were ventilated with a gas mixture containing 15% O_2 and 6% CO_2 in nitrogen at 40 breaths per minute with end-inspiratory and end-expiratory tracheal pressures of 8 and 3 mmHg, respectively, to eliminate any atelectasis occurring during the dissection. The pulmonary artery cannula was connected to a perfusion system containing a physiological salt solution containing 5% bovine serum albumin, and perfused for about 5 minutes at flow rate ranging from 5 to 40 ml/min to remove any residual blood left in the lung vessels and to determine the relationship between pulmonary arterial pressure and pump flow rate. The prefusate exited via the severed pulmonary vein. The lungs, still suspended from the cannulas, were then placed in a 41 mm diameter radiolucent plastic cylinder with its axis at the center of a horizontal turntable so that the lungs could be rotated 360 degrees around a vertical axis between the x-ray source and detector without other x-ray-opaque apparatus obscuring the projection images. The airway pressure was set at 6 mmHg, and the salt solution in the reservoir connected to the arterial catheter was replaced by perfluorooctyl bromide (Perflubron), which was allowed to fill the arterial tree at an initial pressure of about 21 mmHg. The Perflubron provided high x-ray contrast for the vessel lumen, and the surface tension at the Perflubron-aqueous interface prevented its entry into the capillary bed. Thus only the arterial vessels were filled. The arterial pressure was then set at 30 mmHg relative to the horizontal center of the x-ray image of the lungs. The lungs were rotated at 1-degree increments to acquire 360 x-ray projection images in approximately 6 minutes. The arterial pressure was then reduced to 21 mmHg, and a second projection data set obtained. The same sequence was repeated at 12 and 5 mmHg. The actual intravascular pressure within each vessel relative to atmospheric pressure at the level of the vessel was obtained from the vessel's vertical distance from the center of the image, the pressure reference level, and the Perflubron density of 1.94g/ml.

2.2 Micro-CT System

The x-ray system included a Fein-Focus FXE/FXT-100.20 x-ray tube with 3 μm focal spot, and an image train consisting of a Thompson TH9438 image intensifier operating in the 17.8 cm input mode. The image intensifier was optically coupled to a SMD 1M15 CCD Camera (Silicon Mountain Design, Inc., Colorado Springs, CO). The source is mounted on a precision rail, with the conical x-ray beam emerging in a horizontal orientation. The image intensifier is mounted on the rail with provision for movement along the beam axis with source-detector distance variable continuously between 10 and 150 cm. Also mounted on the rail, between the source and detector and similarly axially adjustable, is a high-precision micropositioning specimen stage (New England Affiliated Technologies). The lung preparations can be manipulated in space with four degrees of freedom x-y-z-θ. This, along with the small focal spot, allows for variable geometric magnification. All stage and camera operations are under the control of a Pentium-based PC workstation.

The cylinder containing the rat lung was placed in the scanner so that its central axis was about 25 cm from the source. The source to image intensifier distance was approximately 85 cm, yielding a geometric magnification of about 3.5x and a cone beam half-angle for the lung image of less than 5 degrees. Imaging frequency was 30 frames per second with 30 consecutive frames averaged to comprise each stored image. Following projection image acquisition for each image volume, two additional images were obtained. One image was of a phantom consisting of a uniform grid of 1-mm diameter stainless steel ball bearings (bb's) spaced at 15 mm intervals and embedded in a Plexiglas disc. The bb phantom was attached to the image intensifier input surface and the acquired image was used to correct for spatial distortion inherent in the image intensifier. The other image was a flood field image with the lung removed from the beam. The flood field image provided the unattenuated incident x-ray intensity utilized in the reconstruction algorithm and was used to correct for spatial variations in the x-ray beam and/or image intensifier gain and to determine the x-ray attenuation of the absorbing object.

Each 8-bit (gray level intensities ranging from 0 to 255) planar projection image consisted of a 512 x 512 array of pixels. Prior to reconstructing the image volume from the 360 projection images, preprocessing of the individual images was performed in the following steps: (1) image intensifier spatial distortion correction, (2) location of the axis of rotation and projection image cropping to center on that axis, (3) flood-field division to correct for non-uniform illumination intensity and (4) normalization of the intensity between projections to correct for any temporal drift. Spatial distortion correction was performed on each projection image and the flood field image using a bilinear interpolation transformation determined by mapping the uncorrected individual bb center of mass coordinates from the bb phantom image onto their known spatial locations. The rotation axis was determined by the midpoint between the left- and right-most excursions of a high contrast feature in a 2D Radon transform or sinogram using the same row of pixels extracted from each of the 360 projection images. Each projection image and the flood field image was then cropped so that the axis of rotation occupied the central column of pixels. The flood field image, acquired with the same x-ray technique factors (voltage and current) and geometry as the lung projection images, provided the unobscured illumination intensity for each pixel. Thirty frames were averaged to suppress temporal noise (primarily quantum mottle). The spatially corrected, cropped projections were divided by the corrected and cropped flood field image to provide pixel values proportional to x-ray absorption. Finally, three regions of interest (ROIs) that were unobscured by the object in all projections were located. The ratio of the integrated intensity in these ROIs to that

of the same ROIs in the flood field was used to compute a scaling factor for each image. This scaling factor corrected for any temporal drift in the intensity or in ADC gain during image acquisition. These steps resulted in a final preprocessed image size of 497x497 pixels.

Following preprocessing of the projection images, cone-beam filtered back-projection reconstruction was performed on the preprocessed image data to yield an isotropic reconstruction matrix of 497x497x497 voxels representing a volume of approximately 4.0 x 4.0 x 4.0 cm^3 (about 80 μm per pixel). The Feldkamp[6] cone-beam algorithm was utilized to weight the projection data to account for the angle of the incident x-ray beam at each pixel. The weighted projection data was convolution filtered with the Shepp-Logan[7] kernel, along projection image rows perpendicular to the rotation axis. Then, the filtered data was back-projected from every angle to obtain the volumetric reconstruction. The major advantage of the cone-beam reconstruction was that it allowed for isotropic reconstruction of the entire volume from a single 360° scan. This minimized the scan time, which was important for maintaining tissue mechanical properties for the duration of image acquisition.

3. RESULTS AND CONCLUSIONS

3.1 Principal pathway

A surface shaded rendering of a volumetric rat lung reconstruction obtained as described above is shown in the left panel of Figure 1. The right panel of Figure 1 is the portion of the rendered image volume that represents the principal pathway. To identify the principal pathway, the pulmonary artery was followed from the inlet to the tree to the smallest resolvable terminal vessel. This was done by following the path of the larger diameter vessel segment at each bifurcation, starting at the pulmonary artery inlet. The rendered representation of the principal pathway provided in the right panel of Figure 1 was obtained by removing ("pruning") the portion of the tree downstream from the smaller diameter branch segment encountered at each bifurcation.

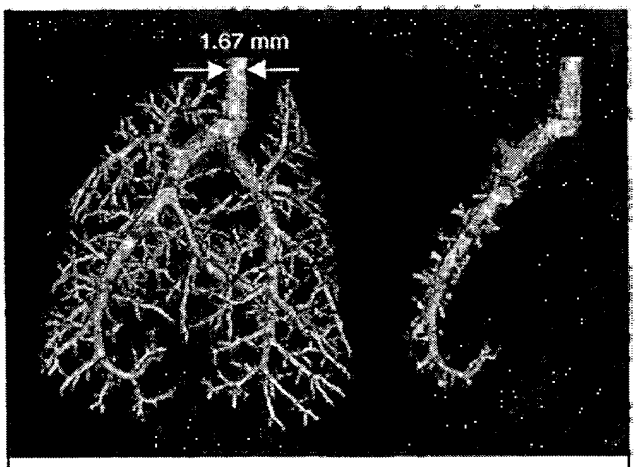

Figure 1. Left: Surface shaded rendering of rat lung with thresholding set to emphasize the contrast enhanced pulmonary arterial tree. Right: Pruned main trunk of the pulmonary arterial tree.

3.2 Arterial tree data

Diameter measurements were obtained by extracting the slice perpendicular to the vessel segment central axis. The CT numbers of the vessel cross section provided a 3D intensity image from which diameter was calculated as described by Johnson, et al.[9]. Each segment length was the 3D straight-line distance along the main trunk axis between consecutive bifurcations. The distance, x, along the principal pathway at which a bifurcation occurred was calculated from the cumulative length of contiguous segments between the current bifurcation and the first bifurcation (x = 0) along the main trunk. The main trunk diameters and lengths and the branch diameters along the principal pathway were measured from image volumes obtained over the range of intravascular pressures from 5 mmHg to 30 mmHg. Figure 2 shows these measurements obtained from the normoxic lung at an intravascular pressure of 21 mmHg. The following mathematical expressions, after Dawson, et al.[10]:

$$D(x,P) = D(0,0)(1-\alpha P)(1-x/Ltot)^c \quad [1]$$

$$D_{BR}(x,P) = D_{BR}(0,0)(1-\alpha P)(1-x/Ltot)^c \quad [2]$$

describe the relationship between trunk diameter, D, branch diameter, D_{BR}, distance, x, and intravascular pressure, P, along the principal pathway, where D(0,0) represents the unstressed (P = 0) trunk inlet diameter. The α term is a measure of vascular distensibility, i.e., the fractional change in diameter due to a change in P. Ltot is the total length of the main trunk if the diameter-distance relationship were extrapolated to zero-diameter, c is the concavity of the taper of the main trunk, and $D_{BR}(0,0)$ is the fitted unstressed diameter of the first branch off the main trunk. The parameter vector for a particular pulmonary arterial tree is the set of parameters obtained by fitting Equations [1] and [2] to the diameter-distance data over the range of intravascular pressures.

The resultant parameter vector included the parameters D(0,0), D_{BR}(0,0), Ltot, c, and α, and an additional parameter, N, that is the number of vessel segments (individual bifurcations) along the main trunk. Equations [1] and [2] were first fit to the normoxic data, resulting in the parameter vector [D(0,0), D_{BR}(0,0), Ltot, c, N, α] of [1.180 mm, 0.566 mm, 38.4 mm, 0.603, 32, 2.5 %/mmHg]. Fitting Equations [1] and [2] to the hypoxic rat data, with only the distensibility parameter free and assuming the normoxic parameter vector values for all other variables, did not provide a statistical improvement on a fit using all free parameters ($p = 0.61$). Therefore, from this comparison, α, was the parameter altered by the hypoxic remodeling (2.5 %/mmHg for the normoxic rat and 1.4 %/mmHg for the hypoxic rat).

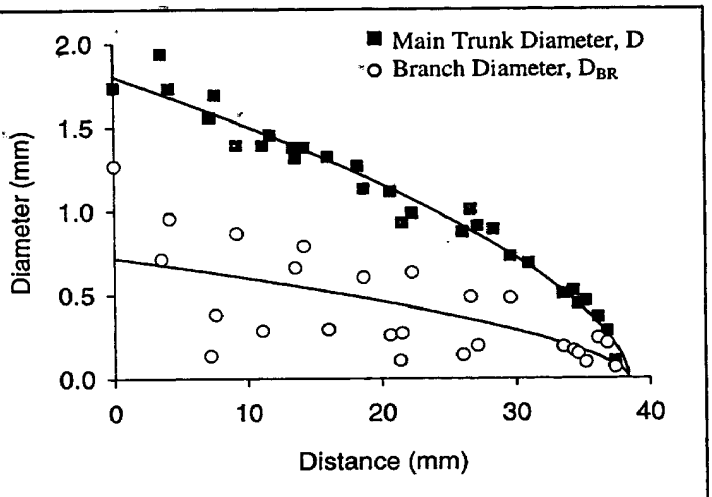

Figure 2. Example of rat pulmonary arterial tree principal pathway diameter, D and D_{BR}, versus distance, x, data from a normoxic rat at 21 mmHg intravascular pressure.

3.3 Hemodynamic model

An important objective of this study was to demonstrate the use of this pulmonary arterial tree parameter vector as an input to a structure-function model based on the self-consistent geometry observed in the pulmonary arterial tree to investigate the influence of the remodeling resulting from chronic hypoxia on hemodynamic function. The hemodynamic consequences of the morphometric parameter vector were evaluated using the recursive self-consistent tree model described by Fredberg and Hoenig[4]. This model exploits the self-consistent structure of the pulmonary arterial tree to allow for computationally efficient hemodynamic evaluation of the resistance, flow and pressure distributions within the vascular tree. Thus, it facilitates understanding of the consequences of differences in vascular morphometry such as occurs between pulmonary normotensive and hypertensive rats.

The self-consistency concept originally applied to pulmonary airways[4] has several attributes that make it an attractive approach for modeling the pulmonary circulation and for taking advantage of the data summarized in the principal pathway morphometric analysis. Conveniently, the biomechanical and geometric parameters obtained from the principal pathway analysis may be used as inputs to a self-consistent tree model whose principal pathway parameterization is statistically equivalent to the real arterial tree. An important feature of the model tree is that geometric and hemodynamic computations are markedly simplified because, based on the self-consistency property, any sub-tree extending from a branch along the principal pathway is statistically equivalent to the portion of the tree subtended by the principal pathway where its diameter equals the branch diameter. The significance of this feature is that a vessel's downstream resistance is a unique function of its generation number (equal to one plus the total number of vessel segments along the principal pathway separating the current vessel segment from the inlet segment, 1 to N for a principal pathway of N contiguous vessel segments). The self-consistent approach is particularly applicable in the context of this study because it retains the asymmetry of the pulmonary arterial tree structure while requiring measurements on a much smaller number of vessel segments than the number comprising the full tree. Consequently, both data collection and the structure-function interpretation of the complex asymmetric pulmonary arterial tree are relatively efficient.

The following is an example of self-consistent tree construction for the simplest case of constant pressure and diameters corresponding to Equations [1] and [2], ignoring the variability in branch diameters and the irregular spacing between bifurcations. The quantity D(0,0)*(1+αP), represented as D(0,P), is taken as the diameter of the inlet vessel segment at the intravascular pressure, P. An initial guess for the L/D ratio is made and the length of the inlet segment is calculated from L/D*D(0,P). Then, at the distance, x, equal to the length of the inlet segment, the next diameter along the principal pathway, D(x,P) is chosen by Equation [1]. The length of this vessel segment is calculated as the product of L/D * D(x,P). This procedure is continued until D(x,P) reaches 30 microns (the smallest measurable vessel diameter in an image volume). If the total number of vessel segments assigned along the main trunk is not equal to N of the parameter vector, the L/D ratio is modified and the main trunk diameters are recalculated until the total number of vessel segments along the model principal pathway equals N.

Once the main trunk diameters and lengths are assigned, the branch diameters are determined. Beginning with the inlet vessel segment, the branch diameter is calculated according to Equation [2] at each distance. The self-consistency property, wherein branches off the principal pathway are exact replicates of downstream portions of the principal pathway, dictates that there are only N unique vessel segments in the entire structure. To achieve this property within the model, the

calculated branch diameters must be compared to the diameters of the segments comprising the main trunk to determine their principal pathway equivalent vessel segment. The main trunk segment providing the minimum absolute difference between its diameter and the calculated branch diameter is selected to represent the branch segment. An example of the principal pathway of this self-consistent model tree is shown in Figure 3 for the normoxic (left) and hypoxic (Right) distensibility estimates. The curves shown in Figure 3 are Equations [1] and [2] fit to the data as shown in Figure 2. The filled boxes and open circles represent the main trunk and branch vessels, respectively, of the model principal pathway.

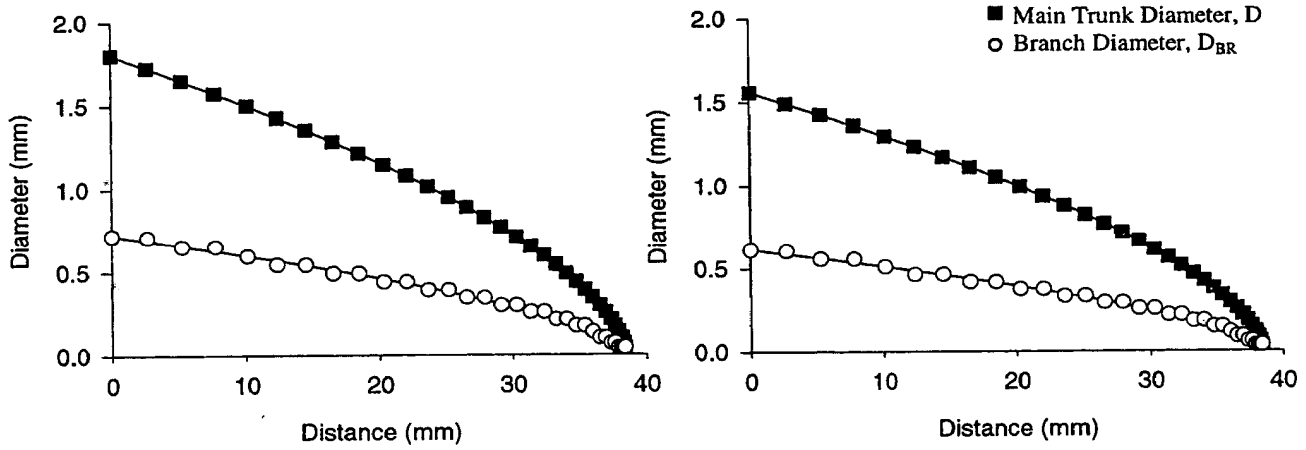

Figure 3. Plot analogous to Figure 2, but for self-consistent model principal pathway diameters, D and D_{BR}, versus distance, x, for normoxic (left) and hypoxic (right) distensibilities at 20 mmHg intravascular pressure. Simulated data were generated from the parameter vector input determined from simultaneously fitting Equations [1] and [2] to the diameter-distance data for all four pressures. Lines represent Equations [1] and [2] fit to normoxic data shown in Figure 2 (left panel) and to the hypoxic rat data (right panel).

A feature of the self-consistent model is that the main trunk and branch segments at the terminal bifurcation along the principal pathway possess identical geometry and, as a result for this constant pressure model, equal Poiseuille resistances. The hemodynamic resistance computation begins at this terminal bifurcation of the principal pathway with a known resistance, and marches toward the principal pathway inlet segment, calculating the series equivalent tree resistance of the portion of the arterial tree downstream from each bifurcation.

To exemplify the hemodynamic analysis for the purpose of this report, self-consistent trees were constructed using the principal pathway parameter vector, as described above, at an intravascular pressure of 20 mmHg and the total downstream resistance at each bifurcation along the principal pathway was calculated. Next, the distensibility was set at the hypoxic value and the diameters for the same intravascular pressure were recalculated. In Figures 4 and 5, these resistances are shown normalized to the total resistance observed in the normoxic model tree. Figure 4 is a graph of normalized resistance versus unstressed vessel segment diameters at both distensibility values which emphasizes that vessels with small diameters (less than about 125 μm) were responsible for over 50% of the total resistance in the self-consistent pulmonary arterial tree model. The results in Figures 4 and 5 indicate that the total tree resistance increased by 90% (from 1 to 1.9) when the distensibility was changed from 2.5%/Torr to 1.4%/Torr. The 90% increase in resistance due to the change in vascular distensibility was attributed to a constant scaling in diameter due to the ratio of distensibility values, that when raised to the fourth power in the Poiseuille resistance calculation resulted in a 1.9 times proportionality between resistances. This preliminary self-consistent tree model provides an example of how the hemodynamic function can be revealed through the principal pathway parameter vector. The model can be further developed to include the heterogeneity present in the data in both branching ratio (branch diameter to main trunk diameter ratio) and segment lengths (branch spacing) along the principal pathway in the study of structure-function relationships exemplified in Figures 4 and 5.

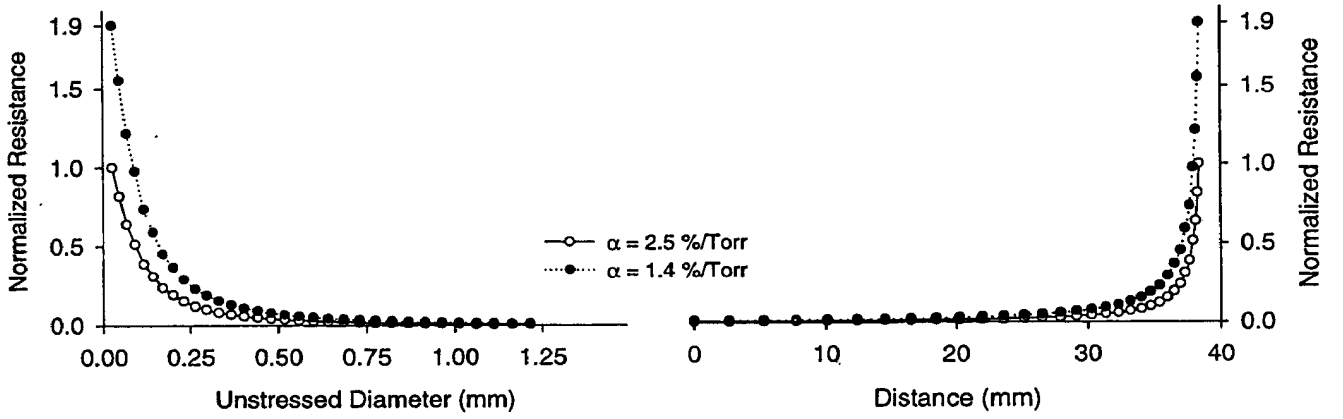

Figure 4. Unstressed main trunk diameter versus normalized resistance for the self-consistent tree model calculated for normoxic ( ) and hypoxic ( ) vascular distensibilities.

Figure 5. Principal pathway distance versus normalized resistance for the self-consistent tree model calculated for normoxic ( ) and hypoxic ( ) vascular distensibilities

ACKNOWLEDGMENTS

Supported by HL19298, the Department of Veterans' Affairs, the Whitaker Foundation, the Falk Medical Trust and the W.M. Keck Foundation.

REFERENCES

1. Horsfield, K. and M.J. Woldenberg, "Diameters and cross-sectional areas of branches in the human pulmonary arterial tree," *The Anatomical Record*, **223**, 245-251, 1989.
2. Huang, W, R.T. Yen, M. McLaurine and G. Bledsoe, "Morphometry of the human pulmonary vasculature," *J. Appl. Physiol.*, **81**, 2123-2133, 1996.
3. Weibel, E.R., *Morphometry of the Human Lung*, Academic Press, 1963.
4. Fredberg, J.J. and A. Hoenig, "Mechanical response of the lungs at high frequencies," *J. Biomech. Eng.*, **100**, 57-66, 1978.
5. Liu, Y.H., E.A. Hoffman, and E.R. Ritman, "Measurement of three-dimensional anatomy and function of pulmonary arteries with high-speed x-ray computed tomography," *Invest Radiol.*, **22**, 28-36, 1987.
6. Feldkamp, L.A., L.C. Davis and J.W. Kress, *J. Opt. Soc. Am.*, **1**, 612, 1984.
7. Shepp, L.A., and B.F. Logan, "The Fourier reconstruction of a head section," *IEEE Trans. Nucl. Sci.*, **NS-21**, 21-42, 1974.
8. Johnson, R.H., H. Hu, S.T. Haworth, P.S. Cho, C.A. Dawson and J.H. Linehan, "Feldkamp and circle-and-line conebeam reconstruction for 3D micro-CT of vascular networks," *Phys. Med. Biol.*, **43**, 929-940, 1998.
9. Johnson, R.H., K.L. Karau, R.C. Molthen and C.A. Dawson, "Exploiting self-similarity of arterial trees to reduce the complexity of image analysis," *Proc. SPIE 3660, Physiology and Function from Multidimensional Images*, 351-361, 1999.
10. Dawson, C.A., G.S. Krenz, K.L. Karau, S.T. Haworth, C.C. Hanger and J.H. Linehan, "Structure-function relationships in the pulmonary arterial tree," *J. Appl. Physiol.*, **86**, 569-583, 1999.

*kkarau@mcw.edu; phone 1 414 384 2000 x41440; fax 1 414 384 0115, Research Service 151, Zablocki VAMC, 5000 W. National Ave., Milwaukee, WI 53295.